Polymer Chemistry

Accepted Manuscript

This is an *Accepted Manuscript*, which has been through the Royal Society of Chemistry peer review process and has been accepted for publication.

Accepted Manuscripts are published online shortly after acceptance, before technical editing, formatting and proof reading. Using this free service, authors can make their results available to the community, in citable form, before we publish the edited article. We will replace this *Accepted Manuscript* with the edited and formatted *Advance Article* as soon as it is available.

You can find more information about *Accepted Manuscripts* in the Information for Authors.

Please note that technical editing may introduce minor changes to the text and/or graphics, which may alter content. The journal's standard Terms & Conditions and the Ethical guidelines still apply. In no event shall the Royal Society of Chemistry be held responsible for any errors or omissions in this *Accepted Manuscript* or any consequences arising from the use of any information it contains.

ROYAL SOCIETY OF CHEMISTRY

www.rsc.org/polymers

Efficiency Assessment on Single Unit Monomer Insertion Reactions for Monomer Sequence Control: Kinetic Simulations and Experimental Observations

*Joris J. Haven,[a] Joke Vandenbergh,[a] Rafael Kurita,[a,b] Jonas Gruber,[b] Thomas Junkers[a,c]**

[a]Polymer Reaction Design Group, Institute for Materials Research (imo-imomec), Hasselt University, Campus Diepenbeek, Building D, B-3590 Diepenbeek, Belgium

[b] Escola Polytécnica da Universidade de São Paulo, Avenida Professor Luciano Gualberto, Travessa 3, nº 380, Butantã - São Paulo, 05508-010, Brazil

[c]IMEC division IMOMEC, Wetenschapspark 1, B-3590 Diepenbeek, Belgium

KEYWORDS. Sequence controlled polymers, single unit monomer insertion, Reversible Addition Fragmentation chain Transfer (RAFT), microreactor, mass spectrometry, kinetic modelling

ABSTRACT

The reaction efficiency of single unit monomer insertion (SUMI) reactions via the reversible addition fragmentation chain transfer (RAFT) method is investigated in detail by determination of obtained product yields of optimized batch and microflow synthesis procedures in combination with kinetic simulations of the radical insertion process. A method is developed to obtain exact concentration information of different SUMI products from calibration of corresponding electrospray ionization mass spectra that are recorded on-line during synthesis. Experimental data show that isolated yields decrease for each subsequent SUMI reaction. This effect is investigated via kinetic modelling to understand which parameters have beneficial or negative influence on the reaction outcome. Although most reaction conditions (such as monomer concentration or radical flux) do not play a considerable role in the obtainable yield of the insertion reaction, the model clearly shows that the propagation rate coefficient must display a strong chain-length dependency in order to explain the experimental observations. When taken into account, the simulations very well fit the experimental data obtained from optimized micoreactor flow synthesis and recommendations for SUMI reactions are formulated. Finally, the optimized SUMI conditions obtained from microreactor experiments and kinetic modelling insights have been applied to upscale the SUMI synthesis reactions in a mesoflow reactor. This demonstrates the simple upscalability of continuous flow reactions and opens the pathway towards future synthesis of longer sequence controlled oligomers.

INTRODUCTION

Since the advent of controlled polymerization the development of highly complex macromolecular materials has reached very high sophistication and today the synthesis of virtually any polymer architecture is in one way or the other accessible, with limitations only being imagination and – in many cases – the economy of processes. Often, synthesis routes are available, but overall yields are low due to extensive reaction steps or tedious product isolation procedures. Lately, one of the last frontiers in polymer chemistry[1,2,3] has started to attract significant attention, namely the so called monomer sequence controlled materials. With such materials, oligomers are synthesized that feature a precise – and more importantly freely selectable – order of monomers in a monodisperse chain. In other words, such materials mimic peptides in all aspects with the only difference being that in place of a peptide bond, other moieties are used to connect the single building blocks. Many different synthesis strategies have been suggested;[4,5] most of them make use of click-like chemistry or reactions as known from step-growth polymerizations. The reason for this choice is simply that addition and condensation reactions allow to add one monomer unit at a time, thus minimizing dispersity of the reaction products. However, also chain growth mechanisms are explored towards sequence controlled materials.[6,7,8,9,10,11,12,13,14] Via controlled radical polymerization techniques, numerous multiblock copolymers have to date been achieved, mostly using acrylates or acrylamides to encode information in the main chain. These polymers show an impressive number of blocks put in order, but are inherently of polymer nature and hence display significant dispersity. At the same time, also advances are made towards achieving monodisperse monomer sequence control via controlled radical polymerization methodologies.[15,16] Such approaches require nothing less than removing – or more realistically – circumventing the statistical nature of radical chain growth.

Moad and coworkers have shown how reversible addition fragmentation chain transfer (RAFT)[17] can be used to create single unit monomer insertion (SUMI) products by utilizing the distinct reactivity differences between various radical adducts in the RAFT pre- and main-equilibria.[18,19] In this way, up to two monomer units could be efficiently inserted into the C-S bond of a RAFT agent. Advantages of this approach were that monodisperse products could be directly obtained, but since growing polymer chains become inevitably successively closer in radical reactivity, the concept is difficult to be pushed beyond creation of dimers. In a similar approach, we demonstrated that one can perform SUMIs with using only acrylates (and thus with monomers of very similar reactivity) by accepting the statistical nature of the reactions, but performing advanced product separation, in which the desired SUMI products are isolated from their by-products (species in which either no monomer or several monomers were built in).[15] With the help of recycling preparative size exclusion chromatography, isolation of SUMI oligomers with up to 4 monomer units and thus (including the RAFT-typical groups) 6 functionalities in precise order was demonstrated (see Scheme 1 for a general reaction scheme).

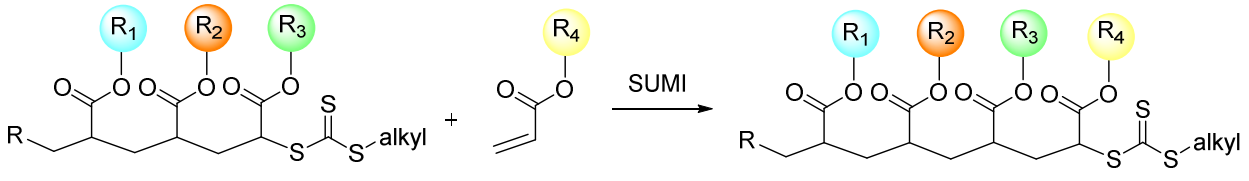

Scheme 1: Single unit monomer insertion reaction using the RAFT process

This approach features several advantages. Monomers can be chosen independent of their characteristic reactivity. At the same time, a broad range of monomers is available. By employing acrylate esters, a virtually infinite number of functional groups can be introduced into the sequence. These monomers are either commercially available, or can be synthesized easily

by esterification. RAFT shows at the same time a high tolerance towards functional groups, allowing to polymerize polar, unpolar or ionic monomers. Thus, monomer ester functionalities can match the known variety of amino acids efficiently. The clear disadvantage of this method is the reaction yield, which is limited by the reaction statistics and by limitations in product isolation. With each growth iteration step, separation on a preparative column becomes more difficult, thus limiting the maximum chain length of the sequence controlled oligomer.

Obviously, isolated yields (after column separation) can be increased when the theoretical yields in the crude product mixture are maximized. Recently, we have shown how such optimization can be carried out in facile fashion using on-line ESI-MS reaction monitoring in combination with continuous flow reactions in a microreactor device.[16] In here, we extract some of the previously published data as well as new optimization results for additional SUMI reactions in combination with kinetic simulations in order to provide an efficiency assessment on the SUMI process, taking differences between theoretical yields in crude reaction mixtures and isolated yields into account. In this way, a deeper understanding of the reaction processes is achieved, which is indispensable for future endeavors towards monomer sequence controlled oligomers with longer chain segments. Moreover, we describe the therefore used mass spectrometric data analysis in detail, giving examples on how exact concentration profiles can be obtained from polydisperse SUMI crude mixtures by on-line mass spectrometry. Further, optimized reaction procedures were used to upscale the synthesis of SUMI products, by changing from the micro- to the mesoscale employing chip-based flow reactors. Concomitantly, the SUMI reactions are modelled via the program package Predici® to shine light on the underpinning processes and to elucidate which reaction conditions are optimal to carry out monomer insertions with highest efficiency. As will be shown, distinct chain-length dependencies are crucial in determining the

individual reaction yields, which is not only interesting from an experimental point of view, but which gives also new insights into chain-length dependent radical propagation, an effect that has been strongly debated in the past and which extent is to-date not even in its order of magnitude precisely known.[20]

EXPERIMENTAL SECTION

Materials.

n-Butyl acrylate (*n*BA, Acros, 99%), *t*-butyl acrylate (*t*BA, Alfa-Aesar, 99%) and 2-ethylhexyl acrylate (EHA, Acros, 99%) were deinhibited over a column of activated basic alumina, prior to use. 1,1'-Azobis(isobutyronitrile) (AIBN, Sigma-Aldrich, 98%) was recrystallized twice from ethanol prior to use. 2-Cyano-2-propyl dodecyl trithiocarbonate (CPD-TTC, Sigma-Aldrich, 97%) was used as received. All solvents used are obtained from commercial sources (Acros and Sigma-Aldrich) and used without further purification.

Characterization.

Purification of products was performed on a **recycling preparative HPLC** LC-9210 NEXT system operated by prepure V1.0 software in the manual injection mode (3 mL) comprising a JAIGEL-1H and JAIGEL-2H column and a NEXT series UV detector using $CHCl_3$ as the eluent with a flow rate of 3.5 $mL \cdot min^{-1}$. Fractions were collected manually (in case of first run purifications) and automatically (for repeated purifications where elution times of fractions are well-known).

NMR spectra were recorded in deuterated chloroform with a Varian Inova 300 spectrometer at 300 MHz for ^{1}H NMR and at 75 MHz for ^{13}C NMR using a Varian probe (5 mm-4-nucleus AutoSWPFG) and a pulse delay of 12 s. NMR spectra were analyzed in MestReNova software.

ESI-MS was performed using an LTQ orbitrap velos pro mass spectrometer (ThermoFischer Scientific) equipped with an atmospheric pressure ionization source operating in the nebulizer

assisted electro spray mode. The instrument was calibrated in the m/z range 220-2000 using a standard solution containing caffeine, MRFA and Ultramark 1621. A constant spray voltage of 5 kV was used and nitrogen at a dimensionless sheath gas flow-rate of 7 was applied. Capillary temperature was set to 275°C. A mixture of THF and methanol (THF:MeOH = 3:2), all HPLC grade, was used as solvent. Spectra were analyzed in Thermo Xcalibur Qual Browser software.

Kinetic modelling simulations have been carried out with Predici (CIT) version. 7.1.0 on an Intel i5 CPU.

Flow reactor setups

The microreactor setup as well as the on-line coupling with ESI-MS have been described previously.[16] The applied mesoreactor setup consisted of a custom built reactor system (Uniqsis Ltd, UK), fitted with a glass chip reactor (internal volume = 2 mL, channel internal diameter = 1 mm) with active mixing geometry channels and an in-line back pressure regulator (BPR, 17 bar). The reactant solution was degassed in situ by nitrogen purging and introduced into the reactor through a Knauer HPLC pump capable of delivering a solution at flow rates between 0.001 and 10 $mL \cdot min^{-1}$. The reactor temperature was controlled via a conventional hotplate equipped with a temperature controller (IKA Laboratory Equipment, RCT basic, temperature range 20 °C to 150 °C). The solution that exits the mesoreactor was collected while cooled in an ice-bath. The setup is shown in the supporting information (SI, Figure S1).

Synthesis

The synthetic batch procedures towards **SUMI-1A**, **SUMI-2AB** and **SUMI-3ABC** have been described previously.[15,16]

On-line Microreactor procedure towards screening SUMI-2AB. has been described previously.[16]

Mesoreactor flow procedure towards SUMI-2AB. A 39 mL solution of 14.194 mmol (2.610 g, 5 equiv) of the monomer 2-ethylhexyl acrylate (EHA), 2.838 mmol (1.345 g, 1 equiv) of macroRAFT agent **SUMI-1A**, 0.113 mmol (0.0186 g, 0.04 equiv) of AIBN was prepared with butyl acetate as reaction solvent. Chemicals were weighted in a glass vial, dissolved in butyl acetate and via a measuring cylinder transferred into a schott bottle connected to the Knauer HPLC pump. The solution was degassed by nitrogen purging for 30 min to remove the oxygen and subsequently employed to the mesoreactor setup. The conditions applied to the mesoreactor were 100 °C and 5 minutes residence time with a HPLC pump flow rate of 0.4 $mL \cdot min^{-1}$. The reaction mixture that exits the mesoreactor was collected in an ice-bath after the in-line back-pressure regulator (BPR, 17 bar) and transferred into an aluminum pan to evaporate excess of solvent and monomer. The crude product mixture was purified via recycling preparative SEC to obtain **SUMI-2AB** as yellowish oil in 48% yield (0.889 g). ^{1}H NMR (300 MHz, $CDCl_3$, δ): 4.98–4.82 (m, 1H, CHCOO, backbone, EHA unit), 4.20–3.94 (br, 4H, $CH_2OC=O$, side chains), 3.35 (t, J = 7.5 Hz, 2H, $CH_2SC=S$, chain end), 2.82–2.66 (br, 1H, CHCOO, backbone, *n*BA unit), 2.50–1.82 (br, 4H, $C\underline{H_2}CHC\underline{H_2}CH$, backbone), 1.75–1.50 (m, 2H, CH_2, *n*BA side chain + 1H, CH, EHA side chain + 2H, CH_2, chain end), 1.46–1.15 (br, 10H, CH_2, side chains + 18H, CH_2, chain end + 6H, CN-C-$(CH_3)_2$), 0.94 (t, J = 7.4 Hz, 3H, CH_3, *n*BA side chain), 0.91–0.80 (br, 3H, CH_3, chain end + 6H, CH_3, EHA side chain). ^{13}C NMR (75 MHz, $CDCl_3$, δ): 221.27, 221.02, 174.30, 170.30, 170.17, 124.18, 68.37, 65.43, 50.55, 49.79, 42.66, 40.63, 40.29, 38.77, 37.62, 35.22, 34.71, 32.02, 31.74, 31.67, 30.59, 30.53, 30.40, 30.37, 29.74, 29.67, 29.55, 29.46,

29.21, 29.01, 27.98, 27.00, 26.96, 26.87, 26.75, 24.97, 23.83, 23.78, 23.09, 22.81, 19.31, 14.25, 14.19, 13.88, 11.10 (SI, Figure S2, S3, S4 and S5). ESI-MS (m/z): 680.38 ($M+Na^+$).

On-line Microreactor flow procedure towards screening of SUMI-3ABC. A 0.20 mL solution of 0.0881 mmol (0.058 g, 1 equiv) of macroRAFT agent **SUMI-2AB** and 0.0070 mmol (1.2 mg, 0.08 equiv) of AIBN with butyl acetate was prepared. A second 1 mL solution of 0.440 mmol (0.056 g, 1 equiv) of the monomer *t*-butyl acrylate with butyl acetate was prepared. Chemicals were weighted in a glass vial with stirring bar and inserted into the glovebox were butyl acetate was added. The solution was stirred for 15 min to remove the residual oxygen. The two solutions were transferred to two gas-tight 1 mL syringes (SGE) and subsequently employed to the microreactor setup. The conditions applied to the microreactor and screened by the on-line MRT/ESI-MS setup are summarized in Table 3 and Table 4.

Mesoreactor flow procedure towards SUMI-3ABC. A 18 mL solution of 1.299 mmol (0.166 g, 1 equiv) of the monomer *t*-butyl acrylate (*t*BA), 1.299 mmol (0.855 g, 1 equiv) of macroRAFT agent **SUMI-2AB**, 0.104 mmol (0.0171 g, 0.08 equiv) of AIBN was prepared with butyl acetate as reaction solvent. Chemicals were weighted in a glass vial, dissolved in butyl acetate and via a measuring cylinder transferred into a schott bottle connected to the Knauer HPLC pump. The solution was degassed by nitrogen purging for 30 min to remove the oxygen and subsequently employed to the mesoreactor setup. The conditions applied to the mesoreactor were 100 °C and 8 minutes residence time with a HPLC pump flow rate of 0.25 $mL \cdot min^{-1}$. The reaction mixture that exits the mesoreactor was collected in an ice-bath after the in-line back-pressure regulator (BPR, 17 bar) and transferred into an aluminum pan to evaporate excess of solvent and monomer. The crude product mixture was purified via recycling preparative SEC to obtain **SUMI-3ABC** as a yellowish oil in 20% yield (0.204 g). ^1H NMR (300 MHz, $CDCl_3$, δ):

4.79–4.63 (m, 1H, CHCOO, backbone, *t*BA unit), 4.20–3.90 (m, 4H, $CH_2OC=O$, side chains), 3.38–3.15 (d t, J = 7.5 Hz, 2H, $CH_2SC=S$, chain end), 2.65–2.41 (b, 2H, CHCOO, backbone, *n*BA and EHA units), 2.42–1.80 (b, 6H, $C\underline{H_2}CHC\underline{H_2}CHC\underline{H_2}CH$, backbone), 1.72–1.52 (m, 2H, CH_2, *n*BA side chain + 1H, CH, EHA side chain + 2H, CH_2, chain end), 1.46–1.41 (tr s, 9H, $OC(CH_3)_3$, *t*BA), 1.42–1.20 (b, 10H, CH_2, side chains + 18H, CH_2, chain end + 6H, CN-C-$(CH_3)_2$), 0.97–0.83 (b, 3H, CH_3, chain end + 3H, CH_3, *n*BA side chain + 6H, CH_3, EHA side chain). ^{13}C NMR (75 MHz, $CDCl_3$, δ): 221.73, 221.88, 221.44, 221.29, 174.82, 174.35, 174.31, 174.08, 169.17, 169.12, 169.05, 168.97, 124.34, 124.28, 82.79, 67.67, 67.61, 65.23, 65.16, 52.14, 52.04, 51.49, 43.48, 42.57, 42.35, 41.58, 41.17, 41.06, 40.68, 40.60, 40.48, 40.43, 38.86, 37.55, 36.63, 36.36, 36.14, 34.67, 34.26, 33.78, 33.03, 32.09, 31.79, 31.66, 30.64, 30.51, 29.80, 29.74, 29.63, 29.52, 29.28, 29.11, 28.02, 27.14, 27.04, 26.90, 26.85, 26.81, 26.76, 23.86, 23.17, 22.87, 19.35, 14.31, 13.94, 11.14. ESI-MS (m/z): 808.25 ($M+Na^+$).

RESULTS AND DISCUSSION

Single Unit Monomer Insertion *via* RAFT

As mentioned above, we have recently demonstrated that the RAFT process can be used for consecutive single unit monomer insertions (SUMI),[15,16] successfully leading to monodisperse acrylate oligomers with precisely defined structure. The synthetic pathway and the exact monomer sequence for the materials under investigation in this contribution is given in Scheme 2. In a first reaction, the initial cyanoisopropyl-functional trithiocarbonate RAFT agent (CPD-TTC RAFT) was reacted with *n*BA to form the **SUMI-1A** product. After purification (see below), **SUMI-1A** was used as macroRAFT agent for subsequent insertion of EHA into **SUMI-2AB** which in his turn was reacted with *t*BA to obtain **SUMI-3ABC**. Note, that throughout this paper, we will use the following systematic naming of SUMI products: the initial digit always refers to the SUMI iteration, thus 1 to the first monomer insertion reaction, 2 for the second, etc. The letters represent the monomer sequence that is obtained in the respective iteration. **SUMI-2ABB** thus hypothetically refers to the second SUMI reaction side product (with **SUMI-1A** as starting material), in which two monomers B were built in.

In our first study, all reactions were carried out in batch and were not fully optimized for maximum product yields. Recently, we also introduced the on-line coupling of a microreactor with soft ionization mass spectrometry (ESI-MS) to optimize reaction conditions (monomer to macroRAFT agent ratio, reaction temperature and residence time) of the **SUMI-2** reaction.[16] In here, we extend this concept to the optimization of the **SUMI-2** and **SUMI-3** reactions and upscaled their synthesis using a mesoflow reactor with an internal volume 100 times larger than the volume of the microreactor. Flow reactors serve hereby not only as a tool to upscale the SUMI reactions; continuous flow, especially in combination with on-line monitoring, allows for

facile kinetic screening and fast optimization of reactions. At the same time, also a better definition of products can be reached in such reactors. The reaction exotherm is quickly dissipated in microfluidic devices, thus leading to a significant reduction in side reactions. In consequence, reaction conditions are better reproducible, batch-to-batch variations are significantly smaller, and overall better microstructures can be expected. Thus, employing continuous flow by itself increases the obtainable yield of the SUMI reaction. At the same time, it can also be assumed that microreactions are – due to their ideal thermal behaviour – much closer to most kinetic modelling studies as no exothermicity and thus temperature change must be considered for this type of reactions. Exactly for this reason, microreactors are often described as ideal kinetic tools, besides their high synthetic potential.

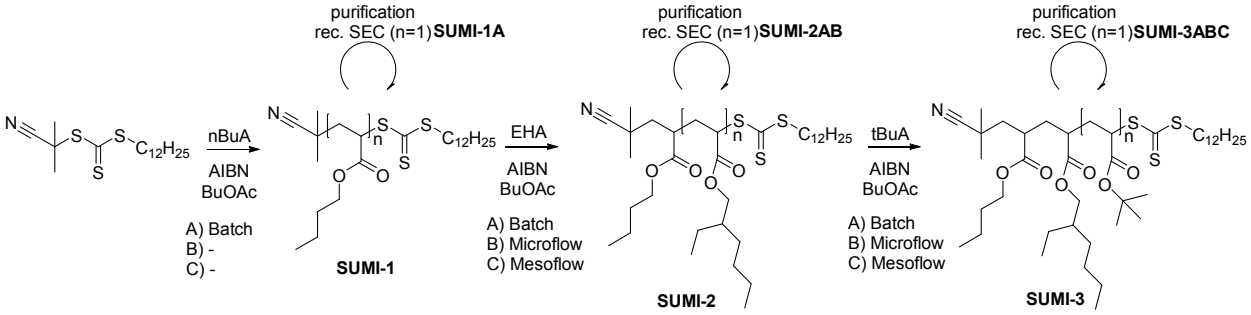

Scheme 2: Synthetic pathway towards sequence controlled **SUMI-1A**, **SUMI-2AB** and **SUMI-3ABC** using radical monomer insertion via RAFT polymerization.

Before discussing the experimental results (and how they were derived), we first focus on the kinetic modelling of the SUMI reactions, as a thorough understanding of the reaction is required to discuss the observed experimental results.

Modelling of SUMI reactions

As described above, single unit monomer insertions are limited in their reaction yield due to the statistical nature of the radical insertion process applied. Important to differentiate is the conversion of a successive SUMI to the desired monomer inserted product (theoretical yield) from the isolated yield of the reaction, which might be significantly different from each other. Obviously, theoretical yields must be kept high in order to allow for most efficient product separations (giving high isolated yields) as column chromatography works the more efficient the less by-products are present in the crude mixture. While these considerations are part of the reaction optimization (see below), it appears worthwhile to investigate SUMI reactions also in a kinetic modelling approach to determine limitations and best operation windows of the insertions. Thus, the reactions as described in the experimental section were modelled using the program package Predici®.

Model description. As most reliable data are available from microreactions, the case of an insertion of one monomer unit into a **SUMI-1** species at 100 °C was adapted following the previously published work. Modelling the insertion into **SUMI-1** instead of initial RAFT agent simplifies the model significantly as no pre-equilibrium stage of the polymerization must be considered. It should be noted that within the scope of this study, the RAFT process is modelled in discrete steps. Thus, one may argue that each SUMI will only take place in a pre-equilibrium since the higher insertions (and hence the unwanted reaction products) would be the result from the main equilbrium. Starting from **SUMI-1**, a much more simplified model is nevertheless obatined since no distinct reactivity difference must be assumed between the initial R group and the acrylate-type oligomers in the SUMI counterparts. The number of parameters to be known is hence largely reduced. The presence of a radical initiator is in any case (be it pre or main

equilibrium) important to model and was consequently taken into account for each insertion. Yet, the impact of these initiator fragments was found to be low. To follow each individual species, no distributions were assumed and all reactions were implemented as elemental reactions. The model consists of individual RAFT equilibria for all possible combinations of radicals and macroRAFT agents between chain length 1 to 4. Termination was considered to occur at the diffusion limit (10^9 L·mol^{-1}·s^{-1} and AIBN of 0.003 mol·L^{-1})[21] according to experiments. Addition of *n*-butyl acrylate was considered, as propagation rate coefficients for this monomer are available with high accuracy.[22,23] No transfer-to-polymer reactions[24] needed to be taken into account due to the limited chain length of all species, allowing to use a pure secondary propagating radical propagation rate coefficient (k_p(SPR)) of 70 000 L·mol^{-1}·s^{-1}. Initiator fragment monomer addition rates were set to be in the same order of magnitude as chain propagation. Radical addition to the macroRAFT agents were set to occur at rates up to 100 times higher than propagation, in line with the observation of chain transfer constants in trithiocarbonate-mediated acrylate polymerizations being generally in the range of 10^2.[25] The full model details are given in the supporting information.

Simulation results

Figure 1 depicts the simulation outcome for the model as described above for an initial [monomer]:[**SUMI-1A**] concentration ratio of 3:1. In Figure 1a, chain-length independent propagation and RAFT addition was assumed, while in Figure 1b chain-length effects are considered. For the chain-length independent model, consumption of all starting material is only achieved at reaching full monomer conversion of the system. The concentration of **SUMI-2AB**,

thus of the desired product, reaches a maximum at around consumption of roughly one equivalent of monomer compared to **SUMI-1A**, which is well in line with expectations. Yet, also significant amounts of **SUMI-2ABB** are present at the same stage already. The high accumulation of **SUMI-2ABBB** at the end of the reaction is indicative that the system under such conditions would feature also species with much higher chain lengths (product **SUMI-2ABBB** represents an accumulation of **SUMI-2ABBB** and all higher chain length derivates). This simulation outcome is not in line with the experimental observation. In experiment, higher fractions of **SUMI-2AB** are found alongside faster conversion of **SUMI-1A** (as can be seen in Figure 1a, **SUMI-1A** has not yet fully depleted even at 90 % of monomer conversion; a fact that can not be confirmed in experiments) and only small amounts of higher chain length species (for detailed discussion of the experimental results, see below).

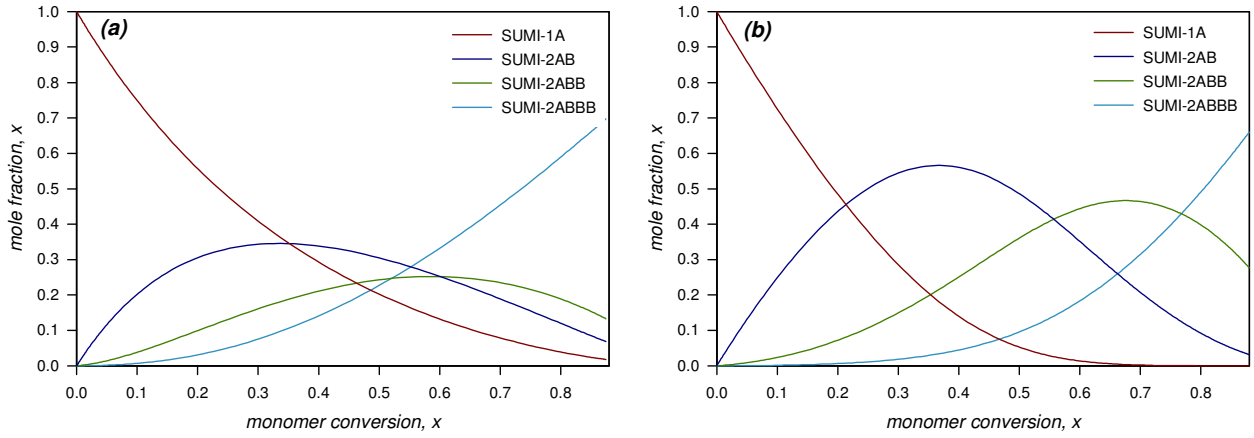

Figure 1: Modelling of the evolution of SUMI products during polymerization assuming (a) a chain-length independent propagation and RAFT addition reaction and (b) under consideration of chain-length effects. For the simulations, a [monomer]:[**SUMI-1**] ratio of 3:1 was assumed for a reaction at 100 °C. **SUMI-2ABBB** represents an accumulation of **SUMI-2ABBB** and all higher chain length derivatives.

Further model refinement was thus required to match the experimental results. Interestingly, changing key parameters such as termination rate coefficients, RAFT addition or intermediate radical fragmentation rate coefficients, monomer concentration (at fixed ratio to **SUMI-1**) or radical flux has very little influence on the outcome of the simulation as shown in Figure 1a and only affects the overall rate of polymerization. The reason why the influence is rather slow is because all shifts are in such case constant and do not lead to a differentiation between the various SUMI products. The distribution between species of different chain lengths is purely given by statistics and in principle a Poisson distribution is obtained.[26] The only way how a deviation from such statistic distribution can be achieved is by implementing a chain-length dependency for the reactions and assigning individual rate parameters to the individual elemental reactions. The key reaction in this respect – a chain-length dependency of the termination rate cannot play a significant role in a well-controlled RAFT system with low AIBN concentrations – is the propagation reaction. A chain-length effect on the propagation reaction has already long been discussed.[20,27,28,29,30,31] Compared to termination, where the change in rate parameters can be essentially assigned to a change in diffusion coefficients,[32,33] a less clear theoretical fundament is given for propagation. Additionally, experiments have shown that any chain-length dependency of propagation is in all likelyhood limited roughly to the first 10 propagation steps and thus hard to follow in polymerizing systems where much higher chain lengths dominate. The exact reason why propagation might be chain-length dependent is not clear and the reader is referred to literature for further information. For the sake of the present study, the reason for the effect is not relevant, only the question if a dependency exists at all is. Nevertheless, Heuts *et al.* had proposed that the rate coefficient for propagation should follow:

$$k_p(i) = k_p(SPR)\left[1 + C_1 \cdot exp\left(-\frac{ln2}{i_{1/2}}\right)(i-1)\right] \quad \text{(Eq. 1)}$$

where k_p(SPR) marks the long-chain limit of k_p (as measured by pulsed-laser polymerization techniques), i the chain length and where C_1 and $i_{½}$ are scaling parameters.[34] Adopting (arbitrary choice) C_1=10 and $i_{½}$=1, the individual rate parameters for $k_p(i)$ (see Table 1) are derived. As can be seen, the predicted variation of the rate is dramatic for the first few reaction steps. Implementation of these coefficients into the model (note that a radical fragment as released from **SUMI-1**, consisting of the original leaving group and one monomer unit, is considered to be of chain length 2) improves the modelling outcome. However only when also the radical addition rate (and the according intermediate radical fragmentation rate) to the macroRAFT is likewise beset with the same chain-length dependency, a modelling result is obtained which is close to the experimental observation (see Figure 1b). While the choice of individual rate parameters is here somewhat arbitrary, the in this way derived results in Figure 1b nicely demonstrate that chain-length effects must clearly play a role in the SUMI reactions when comparing these results with the experimentally derived theoretical yields (see below). Starting material is consumed at a much higher rate compared to the chain-length independent case, and also a better relation between conversion and progressive chain addition is seen. It must be stressed that a similar modelling result as in Figure 1b cannot be reached with the present model if no chain-length dependency is assumed. While on first glance also alternative explanations – such as non-idealities of the RAFT process itself – may be possible to cause a similar effect, only chain-length dependent propagation can really serve as a viable origin of the effect. Any type of termination (including cross-termination of the RAFT intermediate) would lead to significant formation of dead side-products, which is, however, at no time observed experimentally. Likewise, also a strong involvement of AIBN-derived cyanoisopropyl radicals is not observed

experimentally. In addition, the effect of these initiator fragments is even overestimated in the model as equal addition rates to the SUMI products is assumed rather than the reduced rates that are normally adopted. A further potential reaction that may have an effect on the species distribution is a chain-length dependent RAFT intermediate fragmentation rate. However, due to the high temperatures and due to the fact that trithiocarbonates are used (which are known to fragment fast even at low temperatures), an almost ideal RAFT fragmentation can be assumed. The only remaining option would be a chain-length dependent macroradical deactivation, thus the radical addition rate. While such dependence was indeed implemented in the model (due to a constant RAFT chain transfer constant), this alone cannot explain the difference between the the result of Figure 1a and the experimental results. The observed accumulation of **SUMI-2AB** product compared to **SUMI-2ABB** could in such scenario only be explained by increasing deactivation rates with increasing chain length.[35] A decreasing (or constant) k_p with at the same time increasing k_{add} seems to be physically unreasonable as both reactions are similar in nature.

While of course the different SUMI products coexist at any given point in time, better separation of the different concentration profiles is observed. In the example given in Figure 1b (where **SUMI-1A** is used as starting macroRAFT agent), a theoretical yield of 56 % (at exactly $x = 0.33$, note that the absolute maximum is reached slightly above this monomer conversion) is obtained for the desired **SUMI-2AB**. If instead of **SUMI-1A**, **SUMI-2AB** or **SUMI-3ABC** is chosen as start macroRAFT material, yields of resulting **SUMI-3ABC** and **SUMI-4ABCD** insertion products decrease as the chain-length effect between the different species becomes less pronounced ($k_p(2)/k_p(4)=2.66$ vs. $(k_p(4)/k_p(6)=1.71$). For the first single unit monomer insertion starting from **SUMI-2AB**, a theoretical yield of 50 % (for obtaining **SUMI-3ABC**) and starting from **SUMI-3ABC**, a theoretical yield of 46 % (for **SUMI-4ABCD**) is calculated. The trend of

this observed decrease in SUMI efficiency is also observed experimentally (see below), but of course more reliable information on the chain-length dependent k_p would be required to make more accurate theoretical predictions. For the moment, the given numbers only present a trend rather than true expectations. Still, the significant change of $k_p(i)$ is in its order of magnitude required to create the effect and certainly a change in individual propagation rate coefficients in a similar order of magnitude will be realistic. Importantly, as the described product distributions are a direct consequence from the individual rate coefficients rather than the control methodology employed, the herein derived results should be well transferable to other polymerization techniques, such as nitroxide-mediated polymerization[36] or atom transfer radical polymerization.[37] While this hypothesis must be further tested, first results from ATRP-like SUMI reactions currently underway in our laboratories confirm this assumption.

Table 1: Individual propagation rate coefficients used in the modelling of the SUMI reactions following Eq. 1 with C_1=10 and $i_{½}$= 1. Note that the addition of monomer to the radical fragment R-M· was considered to proceed with $k_p(2)$.

k_p**(1)**	770 000 L·mol^{-1}·s^{-1}
k_p**(2)**	420 000 L·mol^{-1}·s^{-1}
k_p**(3)**	245 000 L·mol^{-1}·s^{-1}
k_p**(4)**	157 500 L·mol^{-1}·s^{-1}
k_p**(5)**	113 750 L·mol^{-1}·s^{-1}
k_p**(6)**	91 875 L·mol^{-1}·s^{-1}
$k_p(\infty)$	70 000 L·mol^{-1}·s^{-1}

Recommendations for the SUMI experiments. As mentioned above, the given product distribution does not change much with the experimental conditions and is thus independent on most reaction parameters. This means for the experiment that monomer and RAFT agent concentrations can be chosen freely. Temperature and initiator concentrations may be chosen accordingly to the desired reaction time, however keeping in mind to avoid backbiting and β-scission side reactions which are more pronounced at high temperatures. It is thereby noteworthy to add, that in the modelling roughly 2-3 % termination products are predicted, which is in good agreement to the amount of AIBN put in the model. Hence, the initiator concentration plays for the reaction yield – unless extreme concentrations were considered – no significant role.

A remaining important question is, which monomer to macroRAFT agent ratio is most beneficial for carrying out SUMI reactions. An equimolar range is often proposed as this supposedly leads to a maximum yield of the insertion. As shown above, the theoretical yield is governed mostly by the individual rate parameters, and less by monomer concentration. In fact, when reactions are always stopped at monomer conversions identical to consumption of one equivalent of monomer, very similar product patters are observed, when the initial equivalents of monomer are varied between 1 and 10 (see Table 2).

Table 2: Simulated effect of monomer to **SUMI-1** ratio on the yields of individual products at consumption of one equivalent of monomer.

[Monomer]:[SUMI-1]	1:1	2:1	3:1	4:1	5:1	10:1
***x*(SUMI-1A)**	21%	22%	23%	23%	24%	31%
***x*(SUMI-2AB)**	**58%**	58%	56%	55%	53%	46%
***x*(SUMI-2ABB)**	17%	18%	18%	19%	19%	18%
***x*(SUMI-2ABBB)**	2%	2%	3%	3%	3%	5%

While indeed equimolar conditions result in the highest absolute yield of the first SUMI product (represented in bold in the table), only a very small decrease with increasing monomer equivalents is seen. Only at a ratio of 10:1, a significant reduction of the product yields must be expected. Larger equivalents of monomer are thus recommended for the SUMI reactions as higher monomer concentrations directly translate to increased overall polymerization rates. An additional advantage is given by the fact that truly optimal conditions for maximized yields are not obtained at consumption of one monomer equivalent, but systematically at slighty higher conversions, thus giving a slight advantage of the 2:1 or 3:1 condition over equimolar ratios.

Experimental observations

ESI-MS analysis and isolation of obtained SUMI products

As described above the radical insertion of monomers into a macroRAFT agent is a statistical process, so not only the desired SUMI product is formed, but also multiple insertion by-products. When the crude SUMI products (obtained by RAFT polymerization in batch) are analysed by ESI-MS, the different insertion products can clearly be observed (see Figure 2, left side). Therefore purification using automated recycling size exclusion chromatography (SEC) is required.[38] In recycling SEC, the SUMI product mixture is repeatedly recycled over columns with size exclusion limits from 1000 to 5000 Da. With each additional cycle, the products with different sizes (hydrodynamic volumes) are further separated. The process is fully computer controlled, followed by UV and RI signal detection, and resulting pure product fractions are collected fully automatically. Figure S8 shows the recycling SEC UV trace of consecutive purification cycles of **SUMI-1**, **SUMI-2** and **SUMI-3** reaction products. As can be seen from the figure, separation of SUMI products becomes more tedious upon increasing number of monomer

units in the oligomer chain. Because the hydrodynamic volume of the SUMI species does not increase linearly with increasing chain length, more recycling cycles are required for separation of **SUMI-2** and **SUMI-3**, then for **SUMI-1**. After purification, the pure SUMI products are again analysed with ESI-MS (see Figure 2, right) to confirm the purity of the final monodisperse products. Further, products are also analysed via NMR to confirm their purity. Interestingly, with each monomer insertion, a splitting of some ^{13}C-NMR signals is observed, which can be assigned to formation of diastereomers in the radical addition reaction. No significant diastereoselectivity was observed in the present case, but this feature might find future application in potential stereo-controlled SUMI reactions. Examples of NMR spectra for a SUMI-2 product are given in the SI.

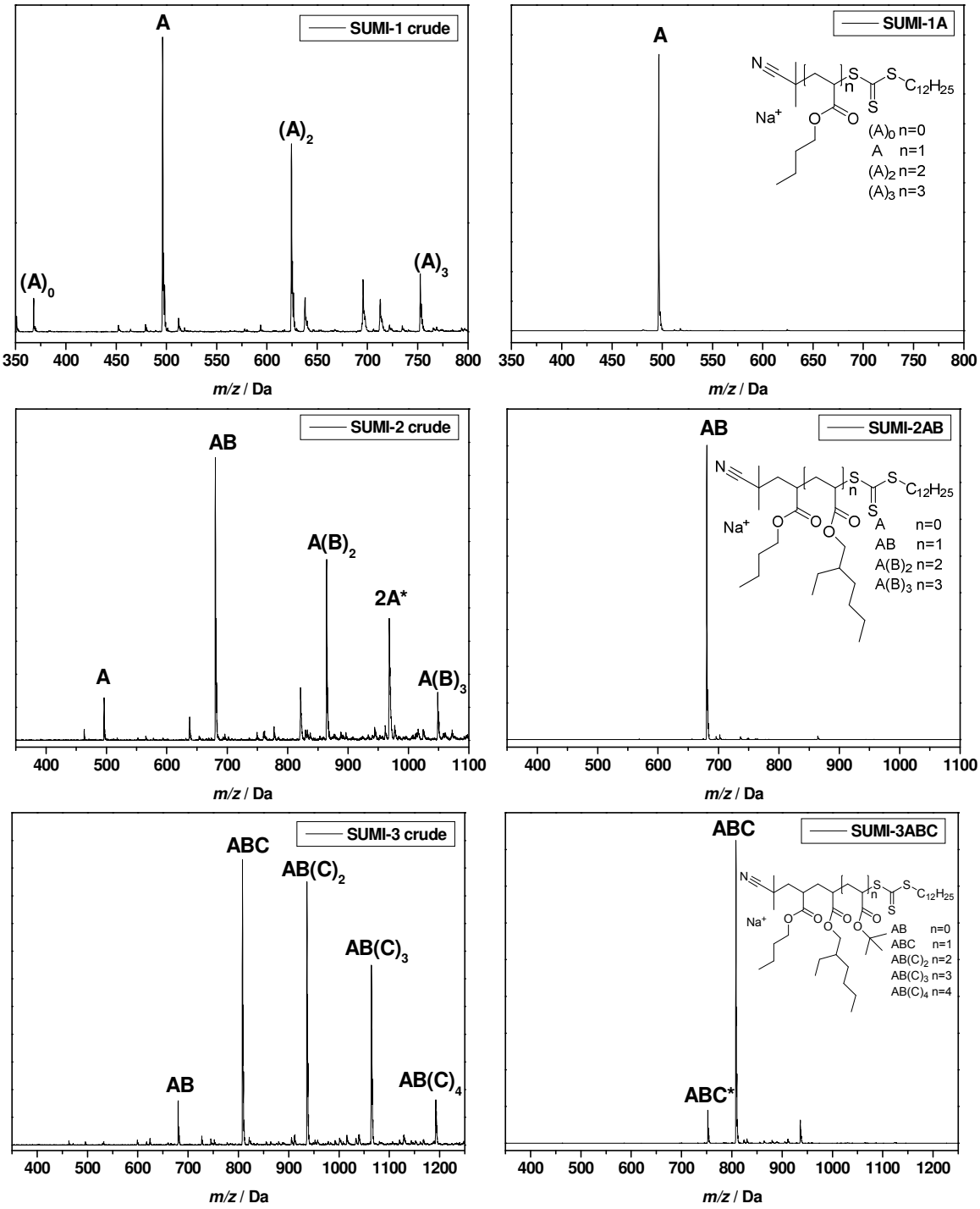

Figure 2: ESI-MS spectra of **SUMI-1**, **SUMI-2** and **SUMI-3** before (left) and after (right) purification with recycling SEC. The species marked with asterisks correspond to an aggregate of 2 A molecules or to an ABC molecule with a hydrolyzed *t*BA unit.

Concentration calibration of ESI mass spectra

The following isolated yields were obtained for the monodisperse batch products: 55% for **SUMI-1A**, 46% for **SUMI-2AB** and 20% for **SUMI-3ABC**. The decreasing yield can be attributed to the predicted loss of efficiency of the SUMI reactions with increasing chain length, but also to the increasing difficulty to separate the different product species from each other. The question thus arises how the isolated yield relates to the theoretical yield in the crude product mixture. As seen in Figure 2, the crude mixture is conveniently analysed by ESI-MS. Mass spectrometry thus offers the opportunity to obtain information on the composition of individual species and hence to directly optimize the reaction parameters towards maximum theoretical yields for each consecutive SUMI reaction.

However, in order to use ESI-MS to determine the yield of the desired SUMI product (species A, AB and ABC in Figure 2) before final isolation, the peak intensities of the different insertion species need to be related to their true molar fractions in the crude SUMI mixtures. Peak intensities in ESI-MS suffer from mass- and ionization bias effects, so they cannot as such be considered as quantitative. In this specific system, it is observed that species containing more acrylate units (hence more polarizable ester moieties) ionize easier than species containing fewer acrylate units. In this case, AB ionizes more readily than A, and ABC ionizes more readily than AB, resulting in apparently increasing peak intensities for equal concentrations. In order to correlate the peak ratios with the true molar fractions, calibration files were prepared for the **SUMI-2** and **SUMI-3** reactions. The **SUMI-1** reaction was left out of consideration for the same reason as why it was excluded from the kinetic simulations, namely because the pre-equilibrium stage alters the kinetic scenario significantly, thus making it difficult to derive clear conclusions from the analysis of this reaction.

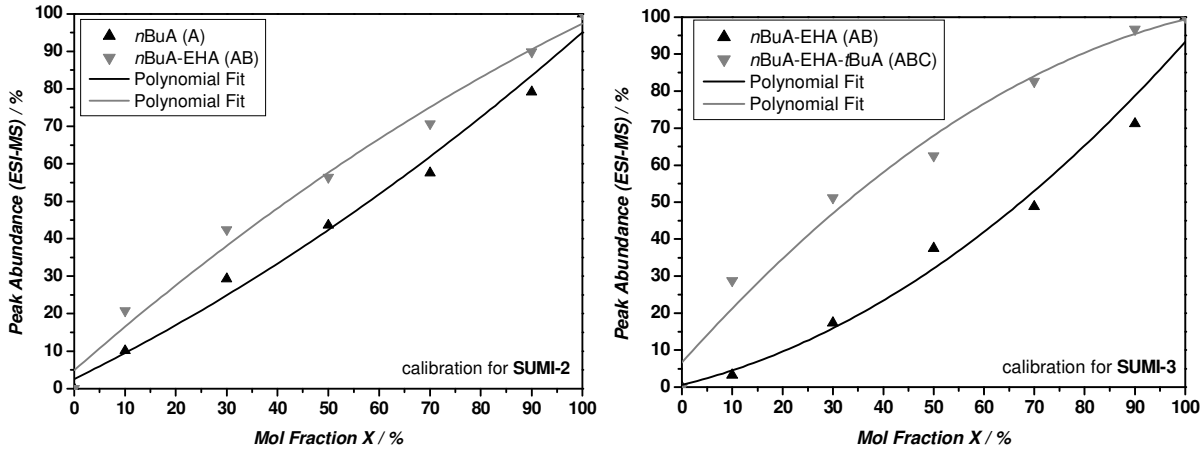

Figure 3: ESI-MS calibration curves for **SUMI-2** and **SUMI-3**, correlating peak abundances of products A, AB and ABC with their true molar ratio.

In a first step to make the calibration file for **SUMI-2**, pure **SUMI-1A** and **SUMI-2AB** were mixed systematically in well-known ratios and the mixtures were measured by ESI-MS. For all molar ratios tested throughout the calibration, the total concentration of the samples was kept constant. Regardless, in the range of concentrations used in this study, no significant impact of the sample solution on the residual mass spectrum must be expected.[39,40] Based on the obtained peak abundances in the mass spectra, calibration curves for species A and AB were determined (Figure 3, left). As can be seen from Figure 3, species A is underestimated relatively to AB, which is in agreement with the fact that AB ionizes more readily due to its extra acrylate unit. In the calibration file, any measured peak abundance for species A or AB can now directly be related to the true molar fraction. It was further also tested if the A:AB peak ratio changed significantly if a certain amount of species $A(B)_2$ was present. But as can be seen from Figure S6

(left) in the Supporting Information, the experimentally measured peak abundances for A and AB stay comparatively constant, regardless of the mole fraction of $A(B)_2$ present. Therefore, the use of the calibration curve in Figure 3 for the more complex SUMI product mixtures, containing several insertion products, appears to yield a good approximation.

For calibration of **SUMI-3**, the same procedure was repeated (Figure 3, right), using mixtures of **SUMI-2AB** and **SUMI-3ABC**. Again experimentally observed peak abundances were compared to true molar AB:ABC ratios and the calibration curves were determined (Figure 3, right). Again, presence of $AB(C)_2$ did not alter the measured peak intensities of AB and ABC too much (Figure S6, right). When comparing calibration curves for **SUMI-2** and **SUMI-3**, the deviation of the measured peak intensities from their true molar fractions, is more severe for the **SUMI-3** calibration. This effect can be explained by the nature of the acrylate unit inserted in the different SUMI reactions. In the case of **SUMI-2**, EHA is used as insertion monomer, which is more apolar than *t*BA, used as model monomer in the **SUMI-3** reaction. Due to this difference in polarity, it is plausible to assume that the ionization bias effect for *t*BA insertions is more pronounced than for EHA insertions, causing this effect in the resulting calibration curves. Another reason for this different ionization behavior might be the lower molar mass of *t*BA compared to EHA. At the same time, this ionization difference also demonstrates that calibrations as shown here are highly sequence-dependent and cannot be used for other monomer combinations. It must also be noted that during optimization experiments (see below), the microflow in-situ injected into the ESI chamber, is of higher concentration (10x-50x) than the manually injected SUMI product mixtures prepared for calibration. However, in this concentration range no additional concentration related bias effects were observed; the only

concentration dependent parameters are the total ion count as well as the maximum injection time to fill the trap.

Optimization utilizing an on-line microreactor/ESI-MS coupling

After the batch reactions have been discussed and calibration files were established with the help of the so-obtained SUMI products, the main focus is in the following put on on-line microreactor/ESI-MS reactions as microflow reactions are expected to yield more stable and reproducible results. The synthesis and optimization of a **SUMI-2** product had been demonstrated before and the description of this step is thus kept short in here (all for the present discussion relevant experimental data is given in the supporting information).[16] By coupling of a microreactor system to an ESI-MS spectrometer, chemical (polymerization) processes are monitored in real time and thus allows for rapid and efficient high-throughput optimization by screening a broad range of reactor residence times, reaction temperatures and reagent ratios (by mixing monomer and macroRAFT solutions from two syringes with individual flow rates). An image and schematic representation of the on-line monitoring setup is shown in the supporting information (Figure S7). Optimization results for the SUMI-2 reaction are given in Table S1 and S2. In conclusion, optimized reaction conditions were identified with 100 °C, a monomer to **SUMI-1A** ratio of 5:1 and a reaction time of 5 minutes (note that a slightly better result was seen for reaction at 110 °C, but for reasons of consistency and in order to reduce the likelihood for thermal elimination reactions, 100°C was chosen). For this case, a total theoretical yield of 59 % for the desired **SUMI-2AB** is identified after ESI calibration, with 11 % remaining starting material, 26 % of **SUMI-2ABB** and 4 % **SUMI-2ABBB** product. The values are in astonishingly good agreement with the simulation results as given in Table 2. This underpins that (*i*) the

assumption of chain-length dependent k_p is very valid (without it the experimental results could not be explained, see discussion above) and (*ii*) that the microflow reactor indeed provides close to ideal reaction conditions that are well represented by simulations. At the same time, it became also evident that the monomer to **SUMI-1** ratio has only little effect on the maximum yield of the product, but only on the rate of reaction (and to some extent distribution of the by-products), which is also well in line with the simulations.

.

SUMI-3ABC was again synthesized in flow by insertion of a *t*-butyl acrylate monomer into the **SUMI-2AB** macroRAFT agent, reaction products are depicted in Scheme 3. Results for the various screening conditions are summarized in Table 3 (ESI-MS peak abundances) and Table 4 (molar ratios from calibration). The temperature was kept constant at 100 °C throughout the optimization experiment since this temperature had been identified as optimal in the **SUMI-2** reactions. Reactor residence times were varied from 2-10 minutes and molar ratios [*t*BA]:[**SUMI-2AB**] from 1:1 to 10:1. Again, only a small variation in product yields was observed when changing the monomer feed ratios, being in good agreement with the theoretical expectations. However, an absolute maximum yield for this reaction was obtained for equimolar ratios between monomer and the starting **SUMI-2AB** product. After 8 minutes reaction time, 34 % of **SUMI-3ABC** was reached, with a significant proportion of unreacted **SUMI-2AB** being left over (41 %). By an increase of the monomer concentration, the amount of unreacted starting material could be reduced, but concomitantly larger amounts of the higher insertion products were obtained. The first case is from a synthetic point of view more attractive as remaining start material is more easily separated from the product and can be reused in following reactions while the higher insertion products usually must be seen as waste. The reason for the slight difference

in reactivity of the **SUMI-3** reaction compared to **SUMI-2** can be explained by the difference in reactivity between EHA and *t*BA, but also by the decreasing chain length dependency. The rather low yield and fast equilibration over the different products in fact hints at the fact that the chain-length dependency of k_p ceases faster with chain length than anticipated in Table 1. Further investigations on this observation are desirable, but could at present not be carried out due to the large experimental efforts that are required for each ESI calibration step. Regardless, in principle the present SUMI experiments allow – provided a broad data basis can be over time gathered – for an assessment of the exact $k_p(i)$ dependency.

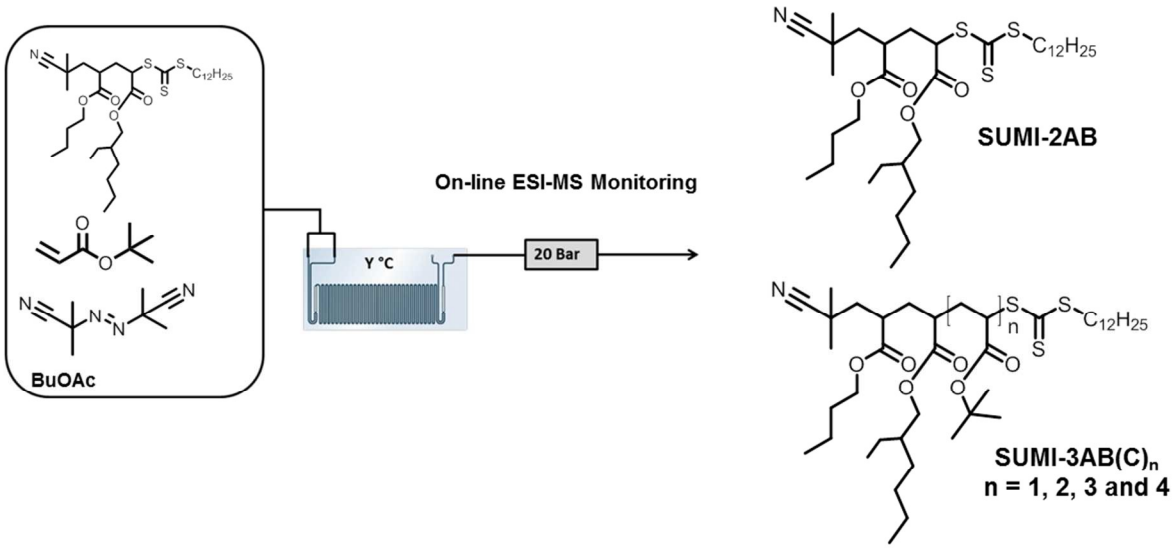

Scheme 3: Schematic representation of the **SUMI-3** insertion reaction in a glass-chip microreactor at 100 °C.

Table 3: Microreactor screening conditions and ESI-MS peak abundances for the synthesis of **SUMI-3ABC**.

Condition	Temp. (°C)	[*t*BA] : [**SUMI-2AB**]	Residence Time (min)	AB (%)	ABC (%)	$AB(C)_2$ (%)	$AB(C)_3$ (%)	$AB(C)_4$ (%)
1	100	10:1	5	8	30	30	22	10
2	100	5:1	5	17	38	30	17	0
3	100	2:1	5	25	43	25	7	0
4	**100**	**1:1**	**8**	**28**	**47**	**21**	**4**	**0**
5	100	2:1	8	16	42	30	10	2
6	100	3:1	8	11	36	32	17	4
7	100	3:1	3	23	45	25	6	1
8	100	5:1	3	18	40	28	11	3
9	100	10:1	2	20	38	26	13	3
10	100	1:1	10	27	48	21	4	0

Table 4: Microreactor screening conditions and molar ratios for all insertion products for the synthesis of **SUMI-3ABC**.*

Condition	Temp. (°C)	[*t*BA] : [**SUMI-2AB**]	Residence Time (min)	AB (%)	ABC (%)	$AB(C)_2$ (%)	$AB(C)_3$ (%)	$AB(C)_4$ (%)
1	100	10:1	5	14	24	30	22	10
2	100	5:1	5	27	28	30	17	0
3	100	2:1	5	37	31	25	7	0
4	**100**	**1:1**	**8**	**41**	**34**	**21**	**4**	**0**
5	100	2:1	8	27	31	30	10	2
6	100	3:1	8	19	28	32	17	4
7	100	3:1	3	35	33	25	6	1
8	100	5:1	3	28	30	28	11	3
9	100	10:1	2	30	28	26	13	3
10	100	1:1	10	41	34	21	4	0

* It is assumed that peak abundances of $AB(C)_2$, $AB(C)_3$ and $AB(C)_4$ match the true molar ratio.

Upscaling of optimized microflow procedures and determination of isolated yields

In the following, the hypothesis that microscale reactions can be easily scaled up is tested. On one hand, upscaling is required to obtain more significant amounts of product, but also with

respect to the determination of isolated yields, an increase in reactant volume is desired. The preparative SEC is associated with considerable dead volume so significant proportions of material are lost if injection loadings are too small, virtually reducing the isolated yield. Thus, by upscaling the reaction, more reliable isolated yields can be determined. Additionally, in Table S3 theoretical and isolated yields for **SUMI2** and **SUMI3** products, synthesized with different setups (batch, micro –and mesoflow) are summarized. It is shown that optimized reaction conditions can easily be transferred from one setup to another, each time resulting in comparable yields. In here, it is observed that regardless of the employed setup, a theoretical yield in the range of 50-59% is obtained for **SUMI-2AB** and a range of 22-34% for **SUMI-3ABC**.[15,16]

Upscaling was achieved by increasing the reactor volume of the flow chips from 19.5 μL to 2 mL, thus by a volume increase of roughly a factor 100. Also, for the larger reactor volume, eluents are fed by HPLC pumps rather than syringe pumps. **SUMI-1A** was again obtained from classical batch experiments, since no further optimization of that reaction is required (high yield reaction and facile separation by SEC). The **SUMI-2** and **SUMI-3** mesoflow reactions were performed under identical conditions as described above for the microreactions. **SUMI-2AB** (condition 11, Table S2) was obtained in 48% (0.889 g) isolated yield after purification by automated recycling SEC whereas **SUMI-3ABC** was obtained with 20% (0.204 g) isolated yield. It should be noted that the runtime of the flow reactions was kept short and samples were collected quickly after reactor stabilization, thus much larger amounts are readily obtained by operation of the flow reactors for several hours. Both crude and pure SUMI products were analysed by ESI-MS (Figure 4). Although some higher insertion products are observed compared to the on-line experimental data for the synthesis of **SUMI-3ABC**, the ESI-MS spectra are overall in good agreement with the earlier ESI-MS spectra (peak abundances) acquired during

the on-line microreactor optimization experiment. The theoretical yields have thus remained in a similar range after upscaling. Especially for **SUMI-2AB** MS results of on-line screening and upscaling are very analogous. The isolated yield (48%) for **SUMI-2AB** corresponds quite well to the ESI-derived theoretical yield of 59% (see above). **SUMI-3ABC** was isolated in 20% yield which is in relatively good agreement with the predicted yield of 34% (Table 4). Isolated yields were thus in both cases somewhat lower than the theoretical yields, which is easily explained by loss of material during purification. Obviously separation becomes more and more difficult with increasing number of monomer units as SEC scales logarithmically with size. Base-line separation of peaks becomes increasingly difficult with each subsequent monomer addition and more and more shoulders in the mass distributions must be cut off to provide pure products. 20 % isolated yield may on first glance be low, but given that already only 34 % theoretical yield could be reached in the crude mixture, this is still a rather satisfying result. Also, the ability to scale the reaction up in flow may not be underestimated. A significant upscale of the reaction is required in order to allow for synthesis of sufficient amounts of **SUMI-3** products. To date, **SUMI-4** products have only been obtained in minute amounts, preventing the push forward to longer oligomer sequences. Batch reactions cannot readily be scaled up due to the relatively high exothermicity of the reactions, and thus continuous flow provides an elegant and easily accessible pathway towards larger product volumes. Recycling SEC can – up to several grams – be used to isolate the various SUMI products and the bottleneck is thus not yet reached.

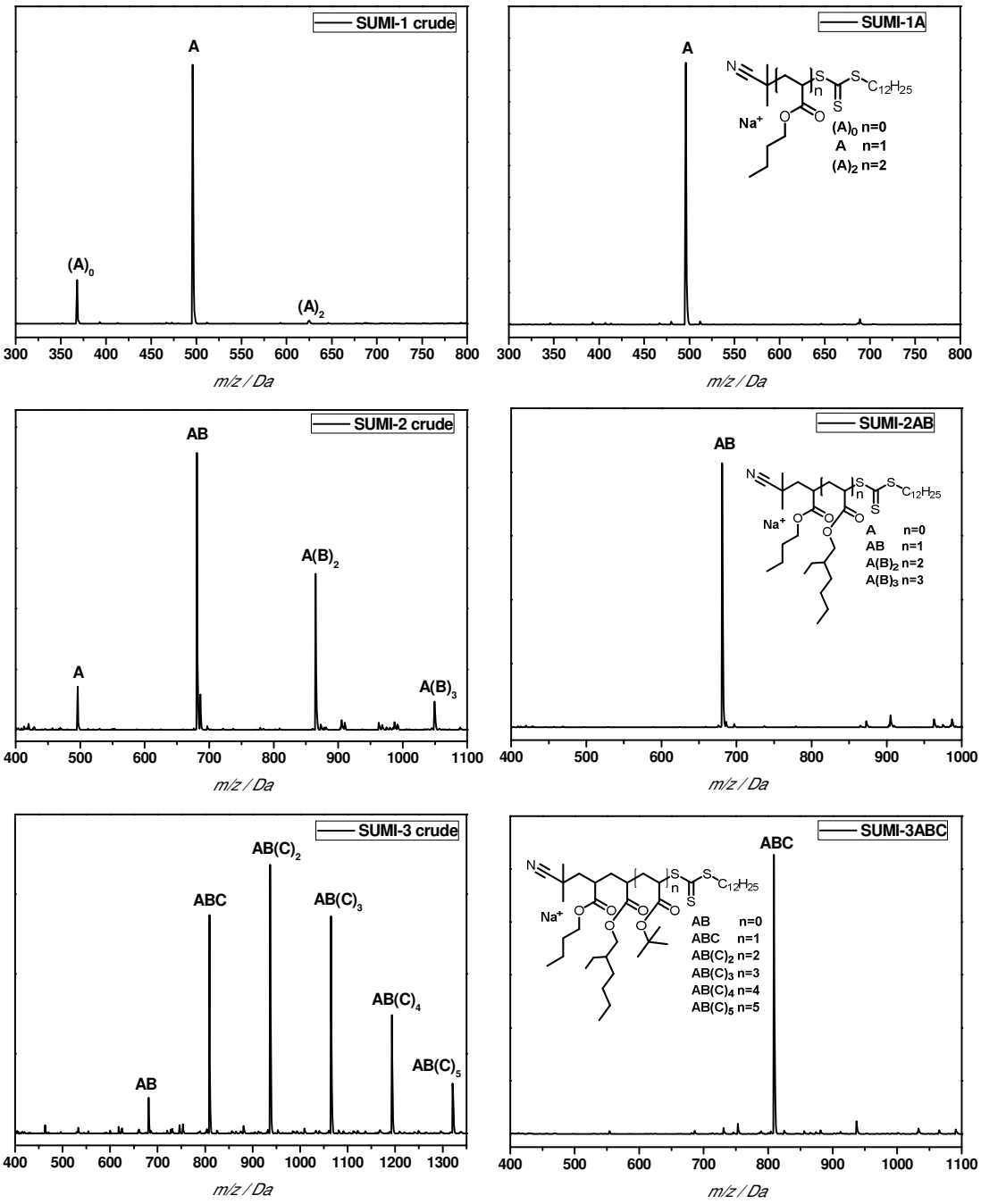

Figure 4. ESI-MS spectra of **SUMI-1**, **SUMI-2** and **SUMI-3** synthesized in mesoflow via RAFT polymerization before (left) and after (right) purification with recycling SEC.

CONCLUSIONS

Single unit monomer insertion reactions have a high potential to provide a variety of sequence controlled oligomers. Elucidation of obtainable yields as presented herein is a crucial step in the development of these reactions since without a good understanding of the involved processes, no meaningful optimization of the reactions may be carried out. At the same time, it is obvious that especially SUMI reactions require a thorough optimization. Isolated yields are – as we have demonstrated by modelling and experiment – comparatively low when going beyond the third monomer insertion. Even lower yields can and must be expected for **SUMI-4** or **SUMI-5** reactions due to the decreasing gap of the individual propagation rate coefficients with each further reaction.

Modelling of the SUMI reactions has shown that most reaction conditions play only a minor role for the success of the insertions. On one hand this is a positive result as it opens a broad range of reaction conditions for SUMI reactions and allows performing SUMIs with short reaction times. Neither monomer concentrations nor radical flux have a distinct impact on the product distributions. On the other hand, it also underpins that SUMIs must be carried out with a somewhat fatalistic attitude. Significant side products must be tolerated and a work-around is difficult if not impossible to achieve.

Further, we could demonstrate that chain-length dependency effects play a crucial role in the SUMI reactions. If equal propagation rate coefficients for each monomer addition step were assumed, much lower theoretical yields of the desired SUMI products are predicted than observed experimentally. In fact, by assuming a strong chain-length dependency (variation of k_p over a factor of 10 within the first 7 propagation steps), simulation results are obtained which are in very good agreement with experimental data from microflow synthesis. It should be noted

though that also the RAFT equilibrium may beset with a chain length dependency, which may have an additional effect on the result.

Microreactions can be efficiently used to optimize the SUMI reactions and the upscale of the reactions is quickly realized by applying the optimized microreactor conditions to mesoflow reactions in a 2 mL glass chip reactor. This is a nice confirmation for the generally assumed simple upscalability of lab-scale continuous flow reactions and certainly shows the pathway towards future developments in synthesis of longer sequence controlled oligomers. Significant efforts still need to be invested to push the technique to a level where also oligomers with chain length above 5 will be available, yet the fundaments for such endeavors (which are ongoing in our laboratories) are now provided.

Supporting Information. Details on the experimental setups, ESI-MS calibration information and complementary experimental data is given in the supporting information.

Corresponding Author

*Corresponding author: Prof. Dr. Thomas Junkers, Hasselt University, Campus Diepenbeek, Building D, B-3590 Diepenbeek, Belgium. Phone + 32 (0)11 26 83 18; Fax: + 32 (0)11 26 83 01. Email: thomas.junkers@uhasselt.be

ACKNOWLEDGMENT

T.J. and J.V. wish to thank the Fonds Wetenschappelijk Onderzoek (FWO) for funding in the framework of the Odysseus scheme and for the FWO postdoctoral fellowship grant of J.V. J.J.H

is grateful for support *via* the BOF funds of Hasselt University. Additionally, support from the European Science Foundation – "Precision Polymer Materials (P2M)" and the Hercules foundation for funding in the framework of the project "LC-MS@UHasselt: Linear Trap Quadrupool-Orbitrap mass spectrometer" is gratefully acknowledged.

REFERENCES

[1] N. Badi and J.F. Lutz, *Chem. Soc. Rev*, 2009, **38**, 3383-3390.

[2] J.F. Lutz, M. Ouchi, D.R. Liu and M. Sawamoto, *Science*, 2013, **341**, 6146, 628.

[3] M. Zamfir and J.-F. Lutz, *Nat. Commun.,* 2012, **3**, 1138;

[4] M. Porel and C.A. Alabi, *J. Am. Chem. Soc.,* 2014, **136**, 38, 13162–13165.

[5] N. Zydziak, F. Feist, B. Huber, J.O. Mueller and C. Barner-Kowollik, *Chem. Commun.*, 2015, **51**, 1799-1802.

[6] J. Vandenbergh, T. de Moraes Ogawa and T. Junkers, *J. Polym. Sci., Part A: Polym. Chem.*, 2013, **51**, 2366-2374.

[7] G. Gody, T. Maschmeyer, P.B. Zetterlund and S. Perrier, *Nat. Commun.,* 2013, 2505.

[8] A. Anastasaki, C. Waldron, P. Wilson, C. Boyer, P.B. Zetterlund, M.R. Whittaker and D.M. Haddleton, *ACS Macro Letters* 2013**, 2**, 10, 896-900.

[9] F. Alsubaie, A. Anastasaki, P. Wilson and D.M. Haddleton, *Polym. Chem.* 2015, **6**, 406-417.

[10] Y. Chuang, A. Ethirajan and T. Junkers, *ACS Macro Lett.*, 2014, **3**, 732-737.

[11] K. Satoh and M. Kamigaito, *Chem. Rev.,* 2009, **109**, 5120–5156.

[12] S. Ida, T. Terashima, M. Ouchi and M. Sawamoto, *J. Am. Chem. Soc.*, 2009, **131**, 10808.

[13] M. Zamfir and J-F. Lutz, *Nat. Commun.*, 2012, **3**, 1138.

[14] K. Satoh, S. Ozawa, M. Mizutani, K. Nagai and M. Kamigaito, *Nat. Commun.*, 2010, **1**, 6.

[15] J. Vandenbergh, G. Reekmans, P. Adriaensens and T. Junkers, *Chem. Commun.*, 2013, **49**, 10358–10360.

[16] J. J. Haven, J. Vandenbergh and T. Junkers, *Chem. Commun.*, 2015, **51**, 4611–4614.

[17] J. Chiefari, Y. K. Chong, F. Ercole, J. Krstina, J. Jeffery, T. P. T. Le, R. T. A. Mayadunne, G. F. Meijs, C. L. Moad, G. Moad, E. Rizzardo, S. H. Thang, *Macromolecules*, 1998, **31**, 5559.

[18] S. Houshyar, D.J. Keddie, G. Moad, R.J. Mulder, S. Saubern and J. Tsanaktsidis, *Polym. Chem.,* 2012, **3**, 1879–1889;

[19] G. Moad, C. Guerrero-Sanchez, J.J. Haven, D.J. Keddie, A. Postma, E. Rizzardo and S.H. Thang in *Sequence-Controlled Polymers: Synthesis, Self-assembly and Properties*, Ed..J.-F. Lutz, T.Y. Meyer, M. Ouchi and M. Sawamoto, ACS Symposium Series; American Chemical Society, Washington, DC, 2014, Vol. 1170, ch. 9, pp. 133-147.

[20] O.F. Olaj, M. Zoder, P. Vana, A. Kornherr, I. Schnoll-Bitai and G. Zifferer, *Maromolecules* 2005, **38**, 1944–1948.

[21] T.Junkers, *J. Polym. Sci. Polym. Chem.* 2011, **49**, 4154-4163.

[22] J. M. Asua, S. Beuermann, M. Buback, P. Castignolles, B. Charleux, R. G. Gilbert, R. A. Hutchinson, J. R. Leiza, A. N. Nikitin, J.-P. Vairon and A. M. van Herk, *Macromol. Chem. Phys.,* 2004, **205**, 2151–2160.

[23] C. Barner-Kowollik, S. Beuermann, M. Buback, P. Castignolles, B. Charleux, M.L. Coote, R.A. Hutchinson, T. Junkers, I. Lacík, G.T. Russell, M. Stach, A.M. van Herk, *Polym. Chem.* 2014, **5**, 204–212.

[24] T. Junkers and C. Barner-Kowollik, *J. Polym. Sci. Polym. Chem.* 2008, **46**, 7585–7605.

[25] G. Moad, E. Rizzardo and S. H. Thang, Polymer 2008, **49**, 1079–1131.

[26] "Handbook of Radical Polymerization", Eds. T.P. Davis and K. Matyjaszewski, Wiley, 2002, ISBN: 978-0-471-39274-3.

[27] O.F. Olaj, P. Vana, M. Zoder, A. Kornherr, and G. Zifferer, *Macromol. Rapid Commun.* 2000, **13**, 913–920.

[28] R.X.E. Willemse, B.B.P. Staal, A.M. van Herk, S.C.J. Pierik and B. Klumperman, *Macromolecules* 2003, **36**, 9797–9803.

[29] J.P.A. Heuts and G.T. Russell, *Eur. Polym. J.* 2006, **42**, 3–20.

[30] G.Moad, E. Rizzardo, D. Solomon and A.J. Beckwith. *Polym. Bull.,* 1992, **29**, 647-652.

[31] H. Fisher and L. Radom, *Angew. Chem. Int. Ed. Engl.*, 2001, **40**, 1340-1371.

[32] C. Barner-Kowollik, and G.T. Russell, *Prog. Polym. Sci.,* 2009, **23**, 1211-1259.

[33] P. Derboven, D. R. D'hooge, M-F. Reyniers, G. B. Marin and C. Barner-Kowollik, *Macromolecules*, 2015, **48**, 492–501.

[34] J.P.A. Heuts, G.T. Russell, G. B. Smith and A.M. van Herk, *Macromol. Symp.,* 2007, 248, 12–22.

[35] a) E. I. Izgorodina and M. L. Coote , *Macromol. Theory Simul.* 2006, **15**, 394–403; b) N. K. Guimard, J. Ho, J. Brandt, C. Yeh Lin, M. Namazian, J. O. Mueller, K. K.

Oehlenschlaeger, S. Hilf, A. Lederer, F. G. Schmidt, M. L. Coote and C. Barner-Kowollik *Chem. Sci.* 2013,**4**, 2752-2759.

[36] J. Nicolas, Y. Guillaneuf, C. Lefay, D. Bertin, D. Gigmes and B. Charleux, *Prog. Polym. Sci.*, 2013, **38**, 63-235.

[37] K. Matyjaszewski, J. Xia, *Chem. Rev.* 2001, **101**, 2921–2990.

[38] L. Zeng, L. Burton, K. Yung, B. Shushan and D. B. Kassel, *J. Chromatogr. A.*, 1998, **794**, 3.

[39] T. Gründling, M. Guilhaus and C. Barner-Kowollik, *Anal. Chem.* 2008, **80**, 6915–6927.

[40] "*Mass Spectrometry in Polymer Chemistry*" Eds. C. Barner-Kowollik, T. Gruendling, J. Falkenhagen, and S. Weidner, 2011, Wiley-VCH, ISBN-10: 3527329242.

Table of Contents

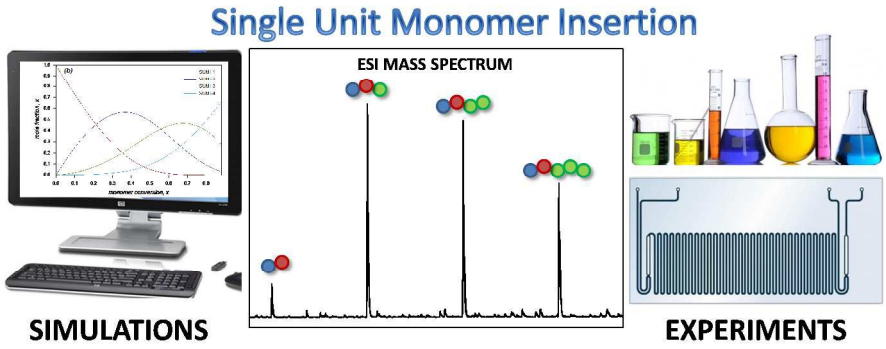

On-line Microreactor/ESI-MS experiments and kinetic simulations on single unit monomer insertions are combined to assess the efficiency of the SUMI process.